

Article

Appraisal of Sulphonation Processes to Synthesize Palm Waste Biochar Catalysts for the Esterification of Palm Fatty Acid Distillate

Shehu-Ibrahim Akinfalabi ¹, Umer Rashid ^{1,*}, Robiah Yunus ² and Yun Hin Taufiq-Yap ³

¹ Institute of Advanced Technology, Universiti Putra Malaysia, 43400 UPM Serdang, Selangor, Malaysia; akinfalabs@gmail.com

² Department of Chemical and Environmental Engineering, Faculty of Engineering, Universiti Putra Malaysia, 43300 UPM Serdang, Selangor, Malaysia; robiah@upm.edu.my

³ Catalysis Science and Technology Research Centre, Faculty of Science, Universiti Putra Malaysia, 43400 UPM Serdang, Selangor, Malaysia; taufiq@upm.edu.my

* Correspondence: umer.rashid@upm.edu.my or umer.rashid@yahoo.com; Tel.: +60-3-97697393

Received: 27 December 2018; Accepted: 24 January 2019; Published: 15 February 2019



Abstract: Palm waste biochar (PWB) catalysts were synthesized as bio-based catalysts using different sulphonation methods. $(\text{NH}_4)_2\text{SO}_4$, ClSO_3H , and H_2SO_4 were applied to functionalize PWB and appraise the discrepancies between the sulfonic agents, as they affect the esterification reaction in terms of fatty acid methyl ester (FAME) yield and conversion while using palm fatty acid distillate (PFAD) as feedstock. The PWB was first soaked in phosphoric acid (H_3PO_4) for 24 h and then pyrolyzed at 400 °C for 2 h in tube furnace. Afterwards, sulphonation was done with different sulfonic agents and characterized with thermo-gravimetric analysis (TGA), Brunauer-Emmett-Teller (BET), Fourier transform infrared (FT-IR), X-ray diffraction (XRD), field emission scanning electron microscopy (FESEM), energy-dispersive X-ray (EDX), and temperature programmed desorption–ammonia (TPD- NH_3). The three synthesized catalysts showed high free fatty acid (FFA) conversions of 90.1% for palm waste biochar-ammonium sulfate (PWB- $(\text{NH}_4)_2\text{SO}_4$), 91.5% for palm waste biochar-chlorosulfonic acid (PWB- ClSO_3H), and 97.4% for palm waste biochar - sulphuric acid (PWB- H_2SO_4), whereas FAME yields were 88.6% (PWB- $(\text{NH}_4)_2\text{SO}_4$), 89.1% (PWB- ClSO_3H), and 96.1% (PWB- H_2SO_4). It was observed that PWB- H_2SO_4 has the best catalytic activity, which was directly linked to its high acid density (11.35 mmol/g), improved pore diameter (6.25 nm), and increased specific surface area ($372.01 \text{ m}^2 \text{ g}^{-1}$). PWB- H_2SO_4 was used for the reusability study, where it underwent eight reaction runs and was stable until the seventh run. PWB- H_2SO_4 has shown huge promise for biodiesel synthesis, owing to its easy synthetic process, recyclability, and high catalytic activity for waste oils and fats.

Keywords: palm waste biochar (PWB) catalyst; sulphonation; PFAD; esterification; FAME

1. Introduction

Concerns about the exploration and exploitation of petroleum fuel, which directly cause environmental pollution, have caused increased consideration for bio-based diesel [1,2]. Biodiesel is environmentally benign, inexpensive, renewable, and sustainable; it therefore becomes a better alternative to petrol-diesel fuel. [3–5]. Biodiesel was initially produced from vegetable oil [6], but it soon raised a food-versus-fuel debate. In order to avert this dilemma, biodiesel has been produced from non-edible oils such as castor oil [7], rubber seed [8], waste animal fats [9], *Jatropha curcas* seeds [10], acidic soybean oil [11], and palm fatty acid distillate (PFAD) [12]. Amongst these non-edible oils, PFAD has exhibited more promising features due its low-cost feedstock and availability in Malaysia.

About 700,000 metric tons of PFAD is produced annually in Malaysia [13]. It has been used in the cosmetic and soap industries in recent years [13]. PFAD also enjoys an added advantage over other saturated/unsaturated fats/oils due to its high miscibility in methanol, which thereby increases its mass transfer, a key component required for high catalytic activity and conversion [1,12]. PFAD consists of the following main fatty acids: 43.2% palmitic acid, 30.1% oleic acid, 7.1% linoleic acid, 3.6% stearic acid, and 1.0% myristic acid. It also contains 10% triglycerides (TG), 3% diglycerides (DG), 1% monoglycerides (MG), and some traces of impurities [13]. PFAD, like all fats, is solid in room temperature and has an free fatty acid (FFA) of about 85 wt%.

Catalysts are extensively used for organic synthesis, especially for the esterification reaction to produce biodiesel. Sodium hydroxide (NaOH), potassium hydroxide (KOH), hydrochloric acid (HCl), and sulfuric acid (H_2SO_4) are conventionally used as basic and acidic homogeneous liquid catalysts since they can complete a reaction in shorter time with better catalytic activity [14]. However, homogeneous basic and acidic catalysts have encountered numerous shortcomings such as soap formation, difficulties with catalyst recovery, equipment corrosion, and waste-water generation, consequently leading to environmental pollution. All these setbacks undermine homogeneous basic and acid catalytic activities [4]. As a result, heterogeneous catalysts have emerged as better alternatives to homogeneous catalysts based on their properties such as their easy catalyst recovery process, their catalyst reusability, their avoidance of instrument/equipment corrosion, and their environmental friendliness [12,14]. Various heterogeneous catalysts have been widely reported such as alkali metal oxides, sulfated oxides, and ion-exchange resins [3,4,6]. Moreover, these commonly used heterogeneous catalysts have some drawbacks such as mass transfer resistance, catalysts leaching, and expensive synthesis process [12]. However, to overcome these prevailing problems, bio-based heterogeneous catalysts with a functionalized acidic group ($-SO_3H$) have emerged and have been reported to be thermally stable; they enhance mass transfer, are cheap and easily accessible, and their continuous usage can solve some problems surrounding solid waste management [15].

Bio-based solid catalysts have recently been exploited from sugarcane bagasse [16], hardwood biochar [17], rice husk [18], and numerous palm parts (palm frond, palm spikelets, palm empty fruit bunch, and palm trunk) [15,19]. Palm waste biochar (PWB) is yet to be exploited, and this forms the basis for this work. About 7.3 m tons of palm waste biochar was processed in 2016, as at March of the same year, 162,519 tons were produced; 256,747 tons were in stock; and 77,005 tons were exported. These facts show the abundance of palm waste in Malaysia [13].

To the best of our knowledge, no study has been done on the appraisal of sulphonation processes to synthesize palm waste biochar (PWB) catalyst for the esterification of PFAD to produce biodiesel. Therefore, the main objective of this work, is to synthesize bio-based PWB catalyst, functionalized with three different sulfonic agents: ammonium sulfate ($(NH_4)_2SO_4$), chloro-sulfonic acid ($ClSO_3H$), and sulfuric acid (H_2SO_4). Another objective is to study the detailed characterization and efficiency of these sulphonated catalysts to determine the highest free fatty acid (FFA) conversion and fatty acid methyl ester (FAME) yield (%) while utilizing waste PFAD as feedstock for biodiesel production.

2. Results and Discussions

2.1. Effect of Soaking in H_3PO_4

The temperature programmed desorption–ammonia (TPD- NH_3) and Brunauer-Emmett-Teller (BET) analyses were done on two different PWB samples: PWB-soaked and PWB. This was done to verify the effect of the H_3PO_4 on the acid distribution, active acid sites, and surface area progression. Figure 1 is an expression of the TPD- NH_3 of the PWB-soaked and PWB where the PWB-soaked peaked at 488 °C indicates a slightly strong acid site, and the PWB had a peak around 260 °C and a very low intensity, which indicates weakness or the absence of a strong acid. The difference is that the PWB-soaked has an advantage of increasing acidity, and also the pore size of the catalyst is sulfonated. As shown in Table 1, the PWB-soaked exhibited a high N_2 desorption owing to its type III isotherm

structure. A type III isotherm is characterized by the adsorption on macroporous or mesoporous adsorbent with a weak adsorbate or adsorbent interactions, having a hysteresis loop at a high-pressure region. This clearly indicates a mesoporous material [20], which may be attributed to the H_3PO_4 used for 24 h impregnation period for effective chemical activation. It is also important to note the pore diameter (D_p) increment from 2 nm to 6.25 nm, for PWB to PWB- H_2SO_4 , respectively. Evident also is the surface area (S_{BET}), which increased from 155.21 to 201.38 ($m^2 g^{-1}$) for PWB and PWB-soaked. The total acidity also shows the discrepancy between the PWB-soaked and PWB, which again points to the effect the H_3PO_4 on the PWB-soaked. As a result of these findings, the PWB-soaked was further sulfonated with three different sulphonated agents: H_2SO_4 , $(NH_4)_2SO_4$ and $ClSO_3H$.

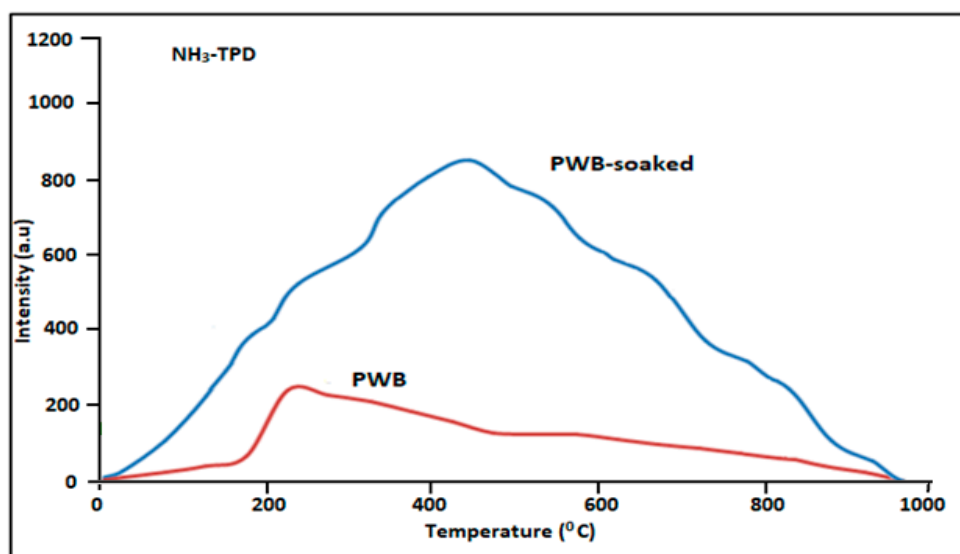


Figure 1. Temperature programmed desorption–ammonia (TPD- NH_3) depicts the effect of soaking palm waste biochar (PWB) in H_3PO_4 .

Table 1. Brunauer-Emmett-Teller (BET) analysis, acid density, free fatty acid (FFA) conversion, and fatty acid methyl ester (FAME) yield of palm waste biochar (PWB), PWB-soaked, sulfuric acid (PWB- $(NH_4)_2SO_4$), chlorosulfonic acid (PWB- $ClSO_3H$), and PWB- H_2SO_4 .

| Sample | ^a S_{BET} ($m^2 g^{-1}$) | ^a V_p ($cm^3 g^{-1}$) | ^a D_p (nm) | ^b NH_3 Acid Density ($mmol g^{-1}$) | ^c FFA Conversion (%) | ^c FAME Yield (%) | ^d Leached Sulfur (%) |
|---------------------|---|--------------------------------------|-------------------------|--|---------------------------------|-----------------------------|---------------------------------|
| PWB | 155.21 | 0.12 | 2 | 0.01 | 33.3 | 29.8 | - |
| PWB-soaked | 201.38 | 0.54 | 3.21 | 6.41 | 54.8 | 51.3 | - |
| PWB- $(NH_4)_2SO_4$ | 270.32 | 0.65 | 4.62 | 8.87 | 90.1 | 88.6 | - |
| PWB- $ClSO_3H$ | 332.87 | 1.61 | 5.11 | 9.63 | 91.5 | 89.1 | - |
| PWB- H_2SO_4 | 372.01 | 0.73 | 6.25 | 11.35 | 97.4 | 95.2 | 1.81 |

^a Measured by BET analysis, ^b measured by TPD- NH_3 analysis, ^c measured by GC-FID analysis, and ^d measured by Carbon, Hydrogen, Nitrogen and Sulphur (CHNS) elemental analysis.

2.2. X-ray Diffraction (XRD) Analysis

The amorphous nature of all the PWBs treated with ammonium sulfate (PWB- $(NH_4)_2SO_4$), sulfuric acid (PWB- H_2SO_4), and chlorosulfonic acid (PWB- $ClSO_3H$) was confirmed by the X-ray diffraction (XRD) analysis. All the observed peaks, as seen in Figure 2, showed weak and broad diffractions of (002) and (101) at 2θ values ranging from 20° to 32° and 35° to 45° .

These key traits are attributable to amorphous carbons, which are characteristically defined by their aromatic sheets since they are randomly oriented [21]. On the other hand, it is observed that the PWB had diffraction peaks around 15° to 19° at 2θ angles, which is different from what is observed for the sulfonated catalysts, and this may be due to the effect of the soaking on the PWB. Our finding is similar to what was reported elsewhere, where their synthesized solid oxide acid catalysts (ZrFeTiO, ZrFeO, and FeTiO) had 2θ angle ranging from 14° to 80° [22].

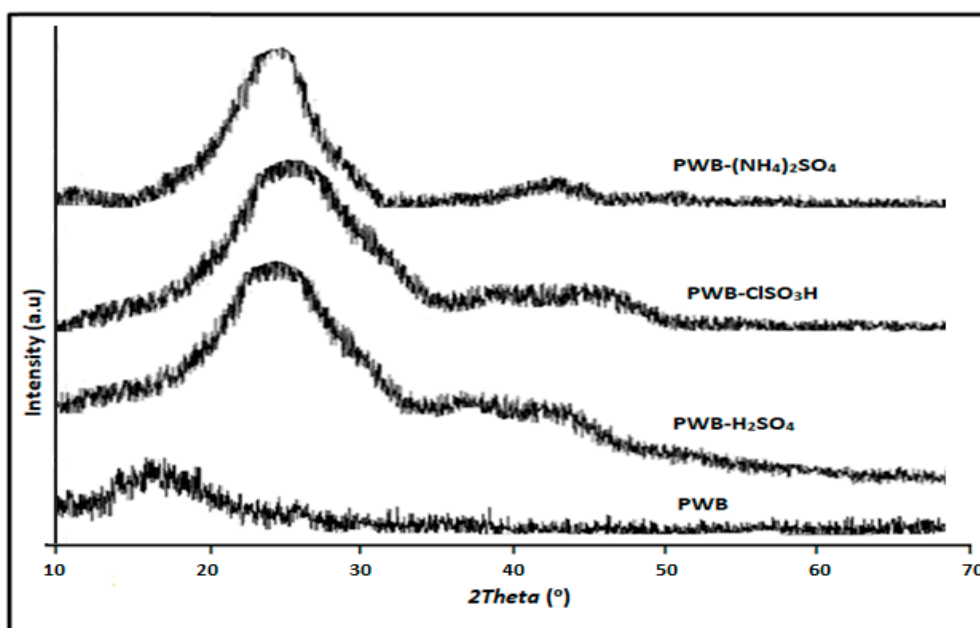


Figure 2. X-ray diffraction (XRD) patterns of PWB, PWB-(NH₄)₂SO₄, PWB-CISO₃H, and PWB-H₂SO₄.

2.3. Fourier Transform Infrared (FT-IR) Analysis

The Fourier transform infrared (FT-IR) spectroscopy was used to investigate the presence of the sulfonic group on the sulfonated PWBs. The obtained infrared spectra depicts a typical adsorption signal for carbon materials. The peaks observed, as shown in Figure 3, at 1172 cm⁻¹ (PWB-(NH₄)₂SO₄), 1167 cm⁻¹ (PWB-H₂SO₄), and 1185 cm⁻¹ (PWB-CISO₃H), are asymmetric vibrational adsorption bands. These adsorption peaks are attributable to the -SO₃H group covalently bonded to the polyaromatic carbon structure of the PWB catalyst. This further confirms the successful sulphonation on the PWB via different sulfonic agents. This finding is similar to the previous reported work [23], where the stretching band recorded at 1175 cm⁻¹ confirmed the sulphonation of PWB. The adsorption peaks observed at 1508 cm⁻¹ for PWB-CISO₃H, 1708 for PWB-(NH₄)₂SO₄, and 1703 cm⁻¹ for PWB-H₂SO₄ are all bands corresponding to the carbonyl (-C=O) group. The last set of peaks seen at 3458 cm⁻¹ for PWB-CISO₃H, 3437 cm⁻¹ for PWB-H₂SO₄, and 3435 cm⁻¹ for PWB-(NH₄)₂SO₄ reflects the presence of hydroxyl group. It is important to note that PWB has no vibrational adsorption band at the -SO₃H region, which shows the absence of the sulfonic functional group. However, it has a band at 3493 cm⁻¹, which corresponds to the hydroxyl functional group band region. The band recorded at 2960 cm⁻¹ for PWB, 2942 cm⁻¹ for PWB-H₂SO₄, and 2951 cm⁻¹ for CISO₃H and 2955 for PWB-(NH₄)₂SO₄ are categorized as phenolic functional groups typical for lignin cellulosic compounds, bonding to the carbon sheets [23].

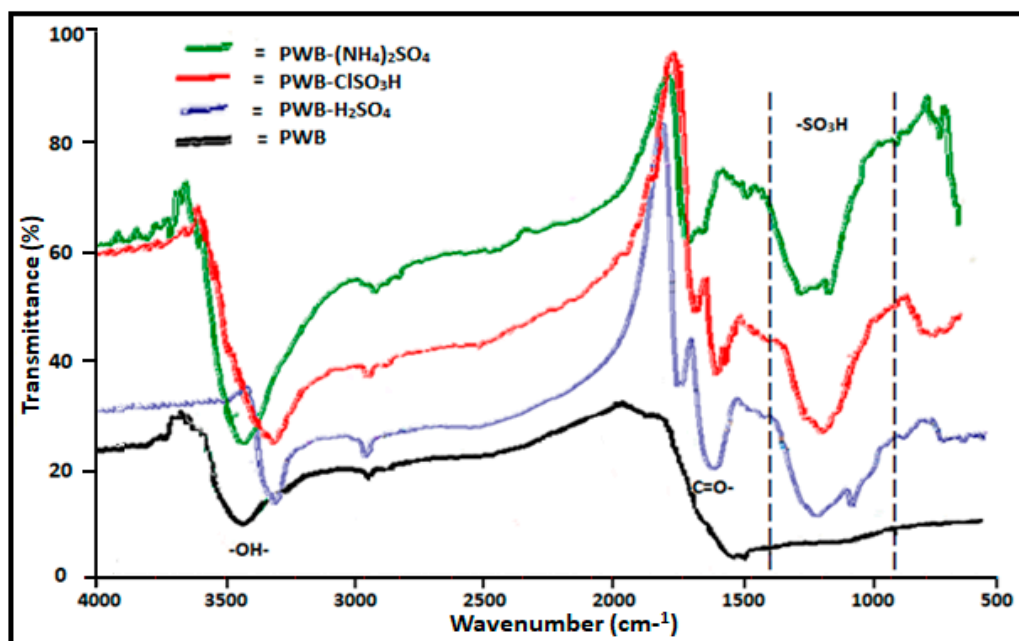


Figure 3. FT-IR spectra of PWB-(NH₄)₂SO₄, PWB-ClSO₃H, and PWB-H₂SO₄.

2.4. Temperature Programmed Desorption–Ammonia (TPD-NH₃) Analysis

The temperature programmed desorption-ammonia (TPD-NH₃) analysis was used to analyze the dispersion/distribution of active acid sites and acidity of the PWB treated with different sulfonic agents and NH₃ used as the probe molecule. As seen in Figure 4, the PWB had two peaks between 280 °C and 450 °C, with a very low TCD signal (intensity/a.u) less than 200 °C, which indicates neither a weak or strong acid but a possible interaction of the NH₃ molecule and the PWB. There are two NH₃ desorption peaks for PWB-H₂SO₄. The first peak around 400 °C suggests the presence of a Lewis acid, whereas the second peak recorded around 810 °C indicates Brønsted acid. This shows that the PWB-H₂SO₄ catalyst has a bi-functional potential [24]. The PWB-ClSO₃H catalyst also recorded two peaks: the first is at 300 °C, which suggests the presence of Lewis acid; the second, which is clearly a Brønsted acid, peaked at 650 °C. The third catalyst PWB-(NH₄)₂SO₄ peaked at 700 °C, which indicated Brønsted acid. The indication of these results is that Lewis acid and Brønsted acid sites were found at their individual desorption peaks ranging from T_{max} of 300 °C and 810 °C. A Brønsted acid, attached via sulphonation onto the PWB, will actively and efficiently catalyze an esterification reaction of PFAD [25]. As presented in Table 1, the acid density recorded for PWB-H₂SO₄ was 11.35 mmol/g, whereas PWB-ClSO₃H recorded 9.63 mmol/g and 8.87 mmol/g for PWB-(NH₄)₂SO₄. Due to this strength in the acid density of PWB-H₂SO₄, it is expected that it will have a better conversion and FAME yield. In comparison, the acid density of Fe(HSO₄)₃ catalyst recorded by Alhassan et al. was 10.5 mmol/g, and their best desorption peak was slightly above 700 °C [25]. This again suggests that synthesized PWB-H₂SO₄ bio-based catalyst had a better performance than most of the acid catalysts.

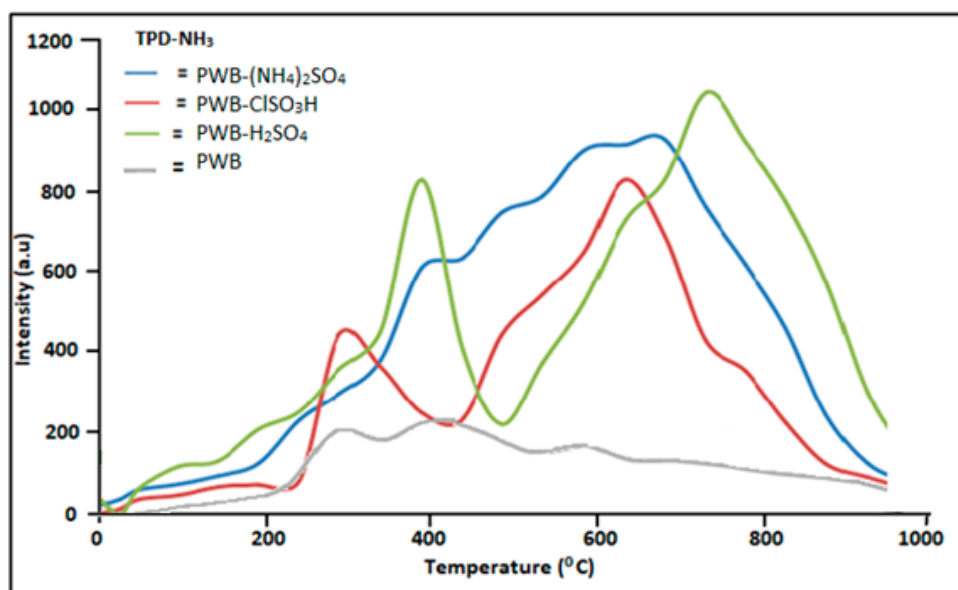


Figure 4. TPD-NH₃ analysis of PWB-(NH₄)₂SO₄, PWB-CISO₃H, and PWB-H₂SO₄.

2.5. Thermo-Gravimetric Analysis (TGA)

The synthesized catalysts were tested for thermal stability using the thermo-gravimetric analysis (TGA). Their thermal stability was investigated and the results presented in Figure 5. The thermal stability was in the order of PWB-H₂SO₄ > PWB-CISO₃H > PWB-(NH₄)₂SO₄. All the three catalysts had an early weight loss between 0 °C to 100 °C, and this is directly due to possible contaminants with lower volatile properties or water loss the water loss [26]. Thereafter, PWB-CISO₃H slowly lost about 20% of its weight around 300 °C where it maintained final stability. PWB-(NH₄)₂SO₄ had the highest weight loss as seen in Figure 5, where it lost about 40% of its weight between 0 °C and 600 °C, and PWB-H₂SO₄ had the best thermal stability of all three catalysts. It lost only about 20% of its total weight between 0 °C and 900 °C. The first 10% could be due to the loss of water molecules, and the other 10% could also be due to the decomposition of the H₃PO₄ and the -SO₃H group [25]; thereafter, it maintained downward degradation.

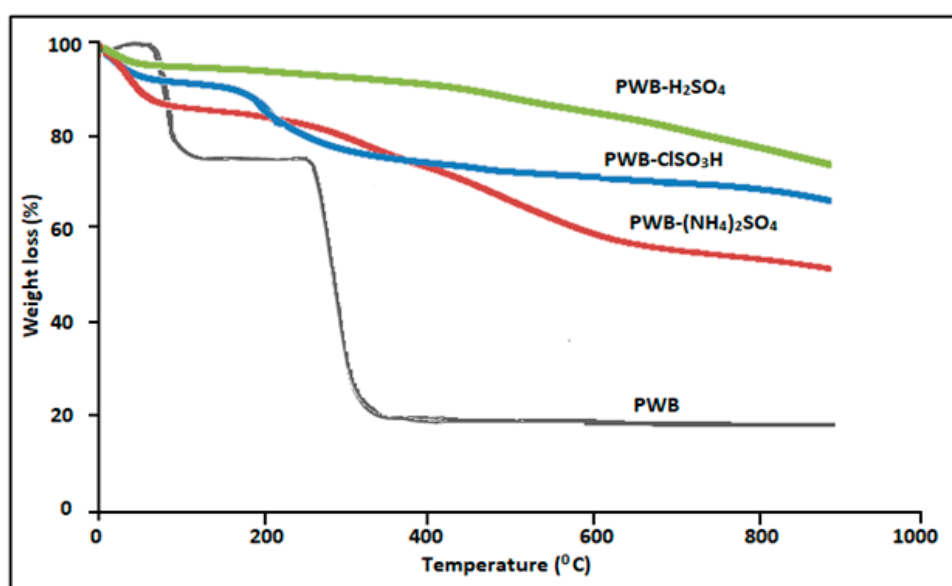


Figure 5. Depiction of TGA analysis of PWB-(NH₄)₂SO₄, PWB-CISO₃H, and PWB-H₂SO₄.

The TGA for the PWB also shows thermal stability between 0 °C and about 100 °C, and when it was degraded from 100 °C to 310 °C, before it maintained stability. This may be due to the lignocellulosic properties of the PWB, which need higher temperature to further degrade. Therefore, PWB-H₂SO₄ is more thermally stable than the other catalysts, and it was selected for further recyclability study.

2.6. BET Surface Area Analysis

The N₂ desorption/adsorption isotherms of PWB-(NH₄)₂SO₄, PWB-ClSO₃H, and PWB-H₂SO₄ have been presented in Figure 6. All the catalysts have shown clear type IV adsorption/desorption isotherms with an HII-type hysteresis loop formed between 0.6 and 0.8 P/P₀, which strongly indicates the presence of a well-developed mesoporous structure that can also be referred to as inkbottle shaped pores [26]. The Brunauer–Emmett–Teller (BET)-specific surface area and BJH pore volumes and pore diameter for PWB-(NH₄)₂SO₄ (), PWB-ClSO₃H, and PWB-H₂SO₄ are 270.32 m² g⁻¹, 0.65 cm³ gm⁻¹, 4.62 nm; 332.87 m² g⁻¹, 1.61 cm³ gm⁻¹, 5.11 nm, and 372.01 m² g⁻¹, 0.73 cm³ gm⁻¹, and 6.25 nm, respectively, as expressed in Table 1. The results showed that the treatment of H₃PO₄ has improved the pore volume and specific surface area of the catalyst compared to PWB (155.21 m² g⁻¹, 0.12 cm³ gm⁻¹, 2 nm) that was neither soaked in H₃PO₄ nor sulphonated. The discrepancy between the pore diameters of the three synthesized catalysts is also important, i.e., PWB-(NH₄)₂SO₄, PWB-ClSO₃H, and PWB-H₂SO₄ are between 4 and 6 (nm), whereas PWB is 2.31 nm, which also indicates a uniform dimension and increased pore diameter of the catalysts [27].

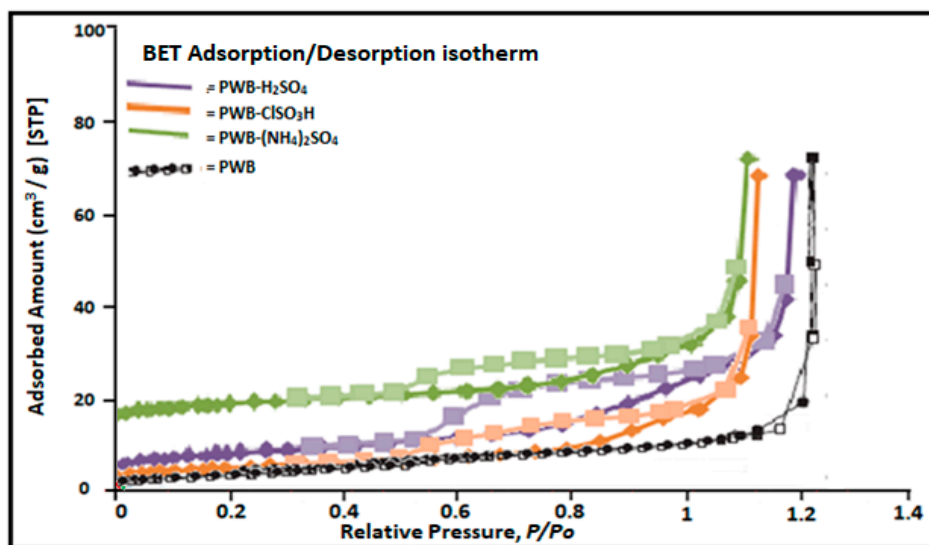


Figure 6. BET analysis of (a) PWB-(NH₄)₂SO₄, (b) PWB-ClSO₃H, and (c) PWB-H₂SO₄.

2.7. Field Emission Scanning Electron Microscopy Analysis

The field emission scanning electron microscopy (FESEM) analysis, as presented in Figure 7, was done to investigate the morphology and surface texture of the synthesized catalysts. It clearly depicts aggregate and irregular structures, confirming the presence of mesopores. The pore sizes of the three catalysts were measured and found to be in the order PWB < PWB-(NH₄)₂SO₄ < PWB-ClSO₃H < PWB-H₂SO₄; this is also confirmed by the EDS and BET analysis presented in Tables 1 and 2. This conforms with the findings reported by Olutoye et al. [22].

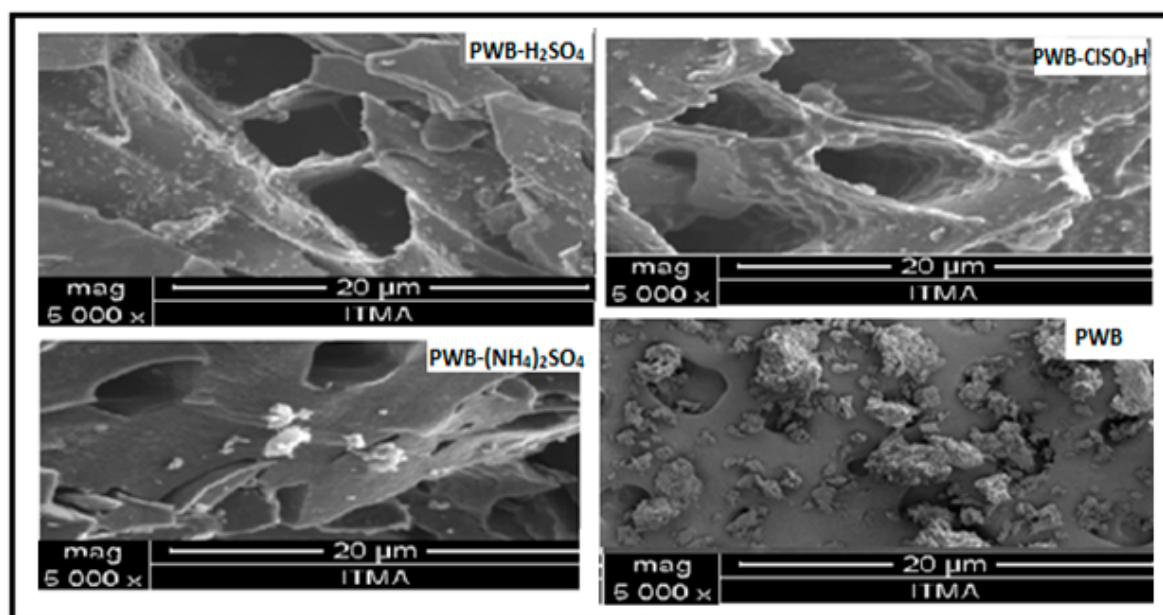


Figure 7. Field emission scanning electron microscopy (FESEM) images of PWB-(NH₄)₂SO₄, PWB-ClSO₃H, and PWB-H₂SO₄.

Table 2. Elemental analysis of PWB, PWB-(NH₄)₂SO₄, PWB-ClSO₃H, and PWB-H₂SO₄ catalysts.

| Sample | C | | O | | S | |
|---|-------------------------|------------------------|-------------------------|------------------------|-------------------------|------------------------|
| | ^a Weight (g) | ^b Atomicity | ^a Weight (g) | ^b Atomicity | ^a Weight (g) | ^b Atomicity |
| PWB | 61.02 | 66.04 | 39.32 | 33.91 | - | - |
| PWB-(NH ₄) ₂ SO ₄ | 60.43 | 70.11 | 17.32 | 11.21 | 3.03 | 1.35 |
| PWB-ClSO ₃ H | 76.19 | 81.74 | 18.57 | 15.46 | 2.81 | 0.67 |
| PWB-H ₂ SO ₄ | 77.36 | 86.45 | 29.65 | 35.22 | 3.16 | 1.31 |

^a Measured using EDS analysis; ^b measured using CHNS elementally analysis.

2.8. PFAD Esterification at Optimized Condition

The FAME yield was calculated with the already established formula (Equation. (1)), and the esterification reaction was carried out using the optimized conditions from our previous study (reaction time of 2 h, reaction temperature of 60 °C, Me-OH: PFAD molar ratio of 9:1, and catalyst loading of 2.5 wt%) [15]. The esterification reaction was run in the sets of three using the PWB-(NH₄)₂SO₄, PWB-ClSO₃H, and PWB-H₂SO₄ catalysts. As can be deduced from Figure 8, PWB-H₂SO₄ has the highest FFA conversion (97.4%) and FAME yield (96.1%), and is our best catalyst in this esterification exercise.

$$\text{FAME yield (\%)} = \frac{\text{weight of produced FAME}}{\text{weight of theoretical FAME}} \times 100 \quad (1)$$

This may be due to the improved pore size, pore volume, or its higher acid density, as a result of the sulfonation, which gives it an added advantage over the other synthesized catalysts. In comparison to our work, Kansedo and Lee, in their work on non-edible sea mango (*Cerbera odollam*) oil to produce biodiesel, utilize the following reaction conditions: 3 h reaction time, 12:1 methanol/oil molar ratio, 8 wt% catalyst concentration, and temperature of 150 °C, and achieved 97.5% conversion [28]. In another study, produced biodiesel via the transesterification of cottonseed oil with a solid catalyst with the following reaction conditions: 8 h reaction time, 2 wt% catalyst loading, 230 °C reaction temperature, and 12:1 methanol/oil molar ratio, had a conversion of >90% [29]. From the above results

and as further highlighted in Table 3, our synthesized PWB-H₂SO₄ catalyst outperformed most of the synthesized catalysts, and therefore PWB-H₂SO₄ has been chosen for further reusability study.

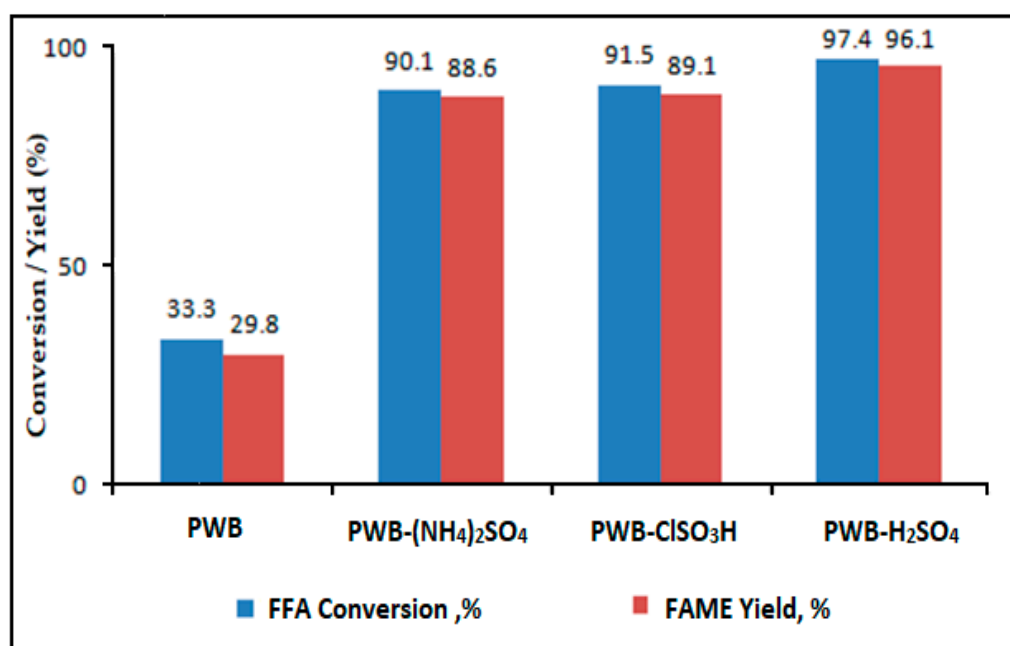


Figure 8. Palm fatty acid distillate (PFAD) esterification reaction at optimized reaction conditions.

Table 3. Performance comparison of different solid basic and acid, bio-based catalysts with that of PWB-H₂SO₄ for biodiesel production.

| Synthesized Catalyst | Reaction Time (h) | Reaction Temperature (°C) | Catalyst Loading (wt%) | MeOH:PFAD Molar Ratio | FAME Yield (%) |
|--|-------------------|---------------------------|------------------------|-----------------------|----------------|
| PWB-H ₂ SO ₄ | 2 | 60 | 2.5 | 9:1 | 96.1 |
| ZrFeTiO [22] | 5 | 170 | 3 | 3:1 | 96.5 |
| MoeMn/g-Al ₂ O ₃ -15 [24] | 4 | 100 | - | 27:1 | 91.4 |
| Fe(HSO ₄) ₃ [25] | 4 | 205 | 1 | 15:1 | 94.5 |
| SO ₄ ²⁻ /ZrO ₂ [28] | 3.0 | 150 | 8.0 | 12:1 | 97.5 |
| SO ₄ ²⁻ /ZrO ₂ [29] | 8.0 | 230 | 2.0 | 12:1 | >90 |
| VOP [30] | 1.0 | 150 | 6.5 | 27:1 | 80 |
| Fe-Zn-1 [7] | 3.0 | 170 | 8.0 | 15:1 | 98 |
| 15 WZ-75 [8] | 3.0 | 200 | 5.0 | 20:1 | 97 |
| SO ₄ ²⁻ /SnO ₂ [9] | 3.0 | 200 | 4.2 | 6:1 | 81 |
| WZ [10] | 4.0 | 250 | 6.7 | 40:1 | >90 |

2.9. PWB-H₂SO₄ Reusability

PWB-H₂SO₄ catalyst was used for the reusability study, and it was investigated through eight (8) successive reaction runs, as presented in Figure 9. PWB-H₂SO₄ catalyst was separated from the mixture and washed using methanol after each esterification run and then dried in an oven set at 80 °C for 12 h. It was afterwards weighed, recorded, and used for the next reaction run using the same reaction conditions. It can be deduced from Figure 9 that the synthesized PWB-H₂SO₄ catalyst recorded a steady and interesting FFA conversion and FAME yield from the 1st reaction run through the 5th run, where it maintained an FFA conversion > 80% and FAME yield > 75% and started to decline through the 7th run. The FFA conversion recorded at the first run was 97.4% and FAME yield of 96.1%, which points to a very high catalytic activity of the synthesized catalyst. The second run had an FFA conversion of 95.3 and yield of 93.1. This trend continued till the 5th run, where the FFA conversion dropped to 82.1% and the FAME yield to 76.3%. It can be recalled (Table 1 and Figure 8) that the PWB was used to esterify PFAD, and the FFA conversion was 33.3% and FAME yield was 29.8%, though there was a large discrepancy, but the 7th run was still able to convert FFA and yield more FAME than the PWB. This may be due to the 1.2% of sulfur-SO₃H left in the PWB-H₂SO₄.

Comparing our results with what was reported elsewhere (Table 3), we can see that our synthesized catalyst outperformed all the listed catalysts and most popular bio-based solid acid catalysts. The PWB-H₂SO₄ shows a highly stable, cheap, and facile synthesis potential.

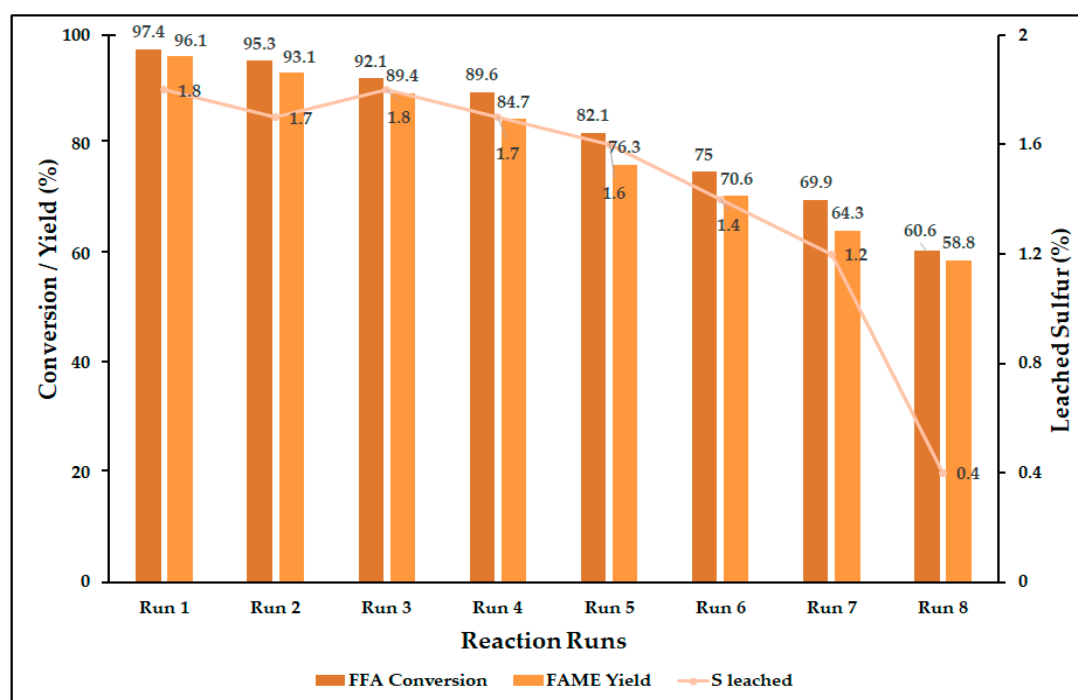


Figure 9. FFA Conversion, fatty acid methyl ester (FAME) yield, and leached sulfur ions during reusability study.

3. Materials and Methods

3.1. Materials

Palm fatty acid distillate (PFAD) and palm waste biomass (PWB) were both obtained from Sime Darby Jomalina, Sdn. Bhd., Malaysia. ClSO₃H (99%), Propan-2-ol (99.97%), *n*-hexane (85%), methanol (99.8%), and ethyl alcohol (96%) were all purchased from Sigma-Aldrich. 98% H₂SO₄ purity and 86% KOH concentration were purchased from J. T. Baker. Chloroform (99.8%), Phenolphthalein and H₃PO₄ (50%) were purchased from Merck & Co (Kenilworth, NJ, USA). Methyl palmitate, methyl linoleate, methyl oleate, methyl heptadecanoate, methyl myristate, and methyl stearate are standards purchased from Fisher Scientific (Waltham, MA, USA) and used for the FAME yield measurement using gas chromatography (GC-FID). All the chemicals used in this work were analytical grade.

3.2. Preliminary Analysis of Palm Waste Biomass (PWB)

The preliminary analysis of PWB, which shows the physico-chemical composition of the starting material (PWB), is presented in Table 4. The physico-chemical composition recorded is cellulose, hemicellulose, lignin, ash, and moisture content, as well as the elemental analysis. Furthermore, the functional groups of PWB has also been presented below.

Table 4. Physico-chemical composition of PWB with selected biomass feedstocks.

| Parameter (% <i>w/w</i>) | Palm Waste Biomass (PWB) |
|--|--------------------------|
| Cellulose | 58.42 |
| Hemicellulose | 21.03 |
| Lignin | 15.32 |
| Ash | 4.18 |
| Moisture content | 5.71 |
| Elemental analysis, dry basis, (% <i>w/w</i>) | |
| Elements (%) | |
| C | 59.65 |
| H | 4.28 |
| N | 1.01 |
| O | 34.19 |
| S | 0.43 |
| P | 0.13 |
| Functional groups (cm ⁻¹) via FTIR | |
| Hydroxyl (-OH) | 3493 |
| Carbonyl (-C=O) | 1499 |
| Phenolic (-OH) | 2960 |

3.3. Experimental Design

Palm waste biomass (PWB) char was divided into two streams: one was treated with ortho-phosphoric acid (H₃PO₄) [PWB-soaked] and the other was not treated [PWB]. They were both calcined under the same conditions (400 °C, 2 h, N₂ flow) and prepared for TPD-NH₃ and BET analysis. Based on the results from TPD-NH₃, (Figure 1), PWB-soaked showed double peak, which signals strong acid sites and higher acid density. Therefore, PWB-soaked was sulfonated with three different sulfonic agents: H₂SO₄, (NH₄)₂SO₄, and ClSO₃H. The resultant sulfonated PWBs (PWB-(NH₄)₂SO₃, PWB-ClSO₃H, and PWB-H₂SO₄) were then taken for TPD-NH₃, BET, FT-IR, XRD, TGA, and FESEM analyses for characterization. After the analyses, based on the best catalytic properties and the FFA conversion/FAME yield via PFAD esterification, the best sulfonated catalyst was chosen for reusability study. The reaction conditions used for the esterification of PFAD was from our previous work. Finally, our findings were compared to published results.

3.4. Preparation of PWB Catalysts and Experimental Methodology

The PWB was dried, ground, and sieved to fine powder (<2 µm). The resulting powder was divided into two; one soaked in ortho-phosphoric acid (PWB-Soaked) for 24 h and the other without soaking (PWB). They were both pyrolyzed differently with crucible tube furnace under nitrogen flow for 2 h at 400 °C. The produced biochar was washed with warm de-ionized water (80 °C) until a pH~7 was achieved, then placed in an oven set at 80 °C to dry for 24 h in order to obtain the soaked palm waste biochar (PWB-soaked) and palm waste biochar (PWB).

3.4.1. Effect of Soaking

The essence of soaking was to screen and confirm that soaking in ortho-phosphoric acid helps to improve pore size and increased acid density from the raw starting material (PWB) that was not treated with orthophosphoric acid. Based on the acid density, active acid sites, pore size/pore diameter, and surface area, the best sulfonated catalyst was selected from the results presented in Figure 1.

3.4.2. Sulphonation Methods

The PWB-soaked was further sulfonated with three different sulfonating agents, namely, sulphuric acid (H₂SO₄), ammonium sulphate [(NH₄)₂SO₄], and chlorosulfonic acid (ClSO₃H). The preparation of

the various sulphonation methods used were adopted and slightly modified from previously reported procedures [31,32].

Sulphonation by Concentrated H₂SO₄

Chemical modification in the form of sulphonation is an essential component in catalysis. This is so because the generation of carboxylic and sulfonic acid groups are made possible, which enhances the acid density and strength of acid group sites attached on the surface of PWB-soaked. Sulfonated PWB was achieved by reacting 4 g of PWB-soaked with 200 mL of concentrated sulfuric acid at 250 °C for 12 h. The resulting sulfonated PWB-H₂SO₄ catalyst was washed, dried, and stored ready to be used for esterification.

Sulphonation by Concentrated (NH₄)₂SO₄

The PWB-soaked was sulfonated by thermally decomposing 4 g in 300 mL 10% of (NH₄)₂SO₄. The mixture was sonicated for 20 min and then heated to 235 °C for 1 h. After cooling, the PWB-(NH₄)₂SO₄ catalyst was washed and allowed to dry overnight in an oven set at 80 °C. The procedure used here is a modified method of what was reported elsewhere [32].

Sulphonation by Concentrated ClSO₃H

The PWB-soaked was also sulfonated using concentrated ClSO₃H in chloroform. 4 g of PWB-soaked was mixed with 200 mL of chloroform for 1 h and was then sonicated for 20 min. Afterwards, 2 g of ClSO₃H was slowly added to the mixture and was refluxed and stirred for 4 h at 70 °C. The resulting solution was washed with ethanol in order for the organic moieties be removed and was then washed with distilled water till a pH of 7 was achieved. The resultant PWB-ClSO₃H catalyst was then filtered and dried in an oven set at 80 °C overnight. The procedure used here is a modified procedure used elsewhere [33].

3.5. Catalysts Characterization

With a scanning rate set at 4 min⁻¹ and range of theta (θ) 10° to 70°, the Shimadzu X-ray diffraction (XRD) 6000 machine (Shimadzu Corporation, Kyoto, Japan) was used to analyze the catalyst's structure and crystallinity. The sulfonated soaked palm cake biochar's (PWB-SO₃H) crystallite size was determined by Scherrer's formula ($D = 0.89\lambda/\beta \cos \theta\beta$), given D as the average crystallite size, λ represents the wavelength of the X-ray beam, β is the full width half maximum (FWHM) values of the peaks, and $\theta\beta$ is the Bragg angle [15]. The FT-IR analysis shows the functionalization of the -SO₃H group as attached on the PWB, using the Perkin Elmer (1725 X) machine. The acid density and active sites distribution was calculated by the NH₃ temperature program desorption (NH₃-TPD) using the Thermo Finnigan TPDRO 1100 series machine and helium as a carrier gas. Using the Mettler Toledo 990, the Thermo-gravimetric analysis (TGA) was performed with differential thermogravimetry (DTG) to ascertain the catalyst thermal stability. The Sorptomatic 1990 series (Thermo Finnigan) instrument (Scientific Instrument Services, Ringoes, NJ, USA) was used for the specific surface area, pore size, pore volume, and pore diameter, for BET analysis. The catalyst's morphology was verified by using a high magnifying field emission scanning electron microscope (FESEM) (JEOL, JSM-6400, Tokyo, Japan).

3.6. Esterification of PFAD

The PFAD was esterified in a 3-necked flask reactor with the addition of a magnetic stirrer, whose function was to keep the mixture continuously stirring during the reaction. Based on our previous study [15], the following reaction conditions were selected: 2 h reaction time, 9:1 molar ratio of methanol-to-PFAD, reaction temperature 60 °C, and 2.5 catalyst weight %. We emptied the mixture in the flask reactor into a centrifuge tube and allowed to cool off to room temperature, at the end of the reaction. It was then centrifuged to attain separation. The upper layer was methanol, then the

PFAD-methyl ester layer and at the bottom was the catalyst. The two upper layers were decanted into a beaker and heated at 60 °C for 1 h for the removal of methanol, and the PFAD-Methyl Ester was measured and recorded. The residue catalyst was washed with methanol (25 mL) and dried for further recyclability study.

3.7. FAME Analysis and FFA Determination

Fatty acid methyl ester (FAME) yield, on the other hand, was calculated from the data gotten from the gas chromatography using EN 14103 method. The GC machine was armed with a flame ionization detector (FID). A highly polar capillary column BPX 70; (length: 60 m, ID: 0.25 mm and capillary: 0.25 mm) was used for separating the various compound compositions of the FAME. Helium was used as the carrier gas, n-hexane as a solvent, and Methyl heptadecanoate as the internal standard [34]. Methyl (stearate, palmitate, myristate, oleate, and linoleate) as reference standards were diluted to 1000 ppm. We set the GC oven to start at 100 °C and increased with temperature rate set at 10 °C min⁻¹ to 250 °C. While the inlet temperature was set at 250 °C, 270 °C was the temperature of the FID. The calculation of FAME yield was done as shown earlier in Equation (1).

Equation (2) was used to calculate the FFA conversions according to the AOCS 5a-40 method [15].

$$\text{FFA conversion (\%)} = \frac{\text{FFA}_f - \text{FFA}_p}{\text{FFA}_f} \times 100 \quad (2)$$

where FFA_f = acid value of the feedstock and FFA_p = free fatty acid value of the FAME.

3.8. CHNS Analysis

Sulfur leaching was analyzed with the CHNS instrument (LECO CHNS-932 spectrometer, Joseph, ST, USA) to determine the amount of leached active -SO₃H sites from PWB-H₂SO₄ catalyst. After each esterification run, 0.05 g of the spent PWB-H₂SO₄ catalyst was collected for sulfur analysis. The elemental analysis of PWB was also performed also using LECO CHNS-932 spectrometer.

4. Conclusions

Conclusively, the different sulphonation methods employed in this study may be used to synthesize bio-based materials as catalysts to produce biodiesel. The PWB sulfonated with H₂SO₄ has shown the best catalytic performance in the conversion of PFAD into FAME, which is directly due to the synthetic process it went through. The initial chemical activation of soaking in orthophosphoric acid helped to increase the pore size and the acidity. PWB-H₂SO₄ had a conversion of 97.4% and yield of 96.1% with an established optimized reaction conditions of 9:1 molar ratio of MeOH:PFAD, time (2 h), temperature (60 °C), and catalyst concentration (2.5 wt%). PWB-H₂SO₄ was also used for eight reaction cycles, which also shows its reaction stability, and the reusability test shows that sulfur leached slowly through the 7th reaction runs. We have shown that bio-based catalysts can be sought from the abundant biomass wastes and can serve as a viable alternative to homogenous conventional catalysts in the production of methyl esters from PFAD and other waste fats/oils, under mild and suitable reaction conditions.

Author Contributions: The conceptualization of this journal article is from S.-I.A. and U.R.; the methodology was designed by S.-I.A.; the writing—original draft was prepared by S.-I.A.; U.R. helped with the editing and supervision; and R.Y. and Y.H.T.-Y. reviewed the manuscript.

Funding: This research was funded by Putra IPS grant at the Universiti Putra Malaysia (UPM), through Putra IPS research grant's project number, GP-IPS/2016/9474900. The authors particularly wish to acknowledge the financial support from Universiti Putra Malaysia (UPM) via Putra IPB grant (GP-IPB/2016/9490400).

Conflicts of Interest: The authors declare no conflict of interest.

References

1. Onoji, S.E.; Iyuke, S.E.; Igbafe, A.I.; Nkazi, D.B. Rubber seed oil: A potential renewable source of biodiesel for sustainable development in sub-Saharan Africa. *Energy Conver. Manag.* **2016**, *110*, 125–134. [CrossRef]
2. Roschat, W.; Kacha, M.; Yoosuk, B.; Sudyoardsuk, T.; Promarak, V. Biodiesel production based on heterogeneous process catalyzed by solid waste coral fragment. *Fuel* **2012**, *98*, 194–202. [CrossRef]
3. Chen, S.Y.; Lao-Ubol, S.; Mochizuki, T.; Abe, Y.; Toba, M.; Yoshimura, Y. Transformation of non-edible vegetable oils into biodiesel fuels catalyzed by unconventional sulfonic acid-functionalized SBA-15. *Appl. Catal. A Gen.* **2014**, *485*, 28–39. [CrossRef]
4. Lee, S.L.; Wong, Y.C.; Tan, Y.P.; Yew, S.Y. Transesterification of palm oil to biodiesel by using waste obtuse horn shell-derived CaO catalyst. *Energy Conver. Manag.* **2015**, *93*, 282–288. [CrossRef]
5. Huang, R.; Cheng, J.; Qiu, Y.; Li, T.; Zhou, J.; Cen, K. Using renewable ethanol and isopropanol for lipid transesterification in wet microalgae cells to produce biodiesel with low crystallization temperature. *Energy Conver. Manag.* **2015**, *105*, 791–797. [CrossRef]
6. Rashid, U.; Anwar, F.; Moser, B.R.; Ashraf, S. Production of sunflower oil methyl esters by optimized alkali-catalyzed methanolysis. *Biomass Bioenergy* **2008**, *32*, 1202–1205. [CrossRef]
7. Santana, G.C.S.; Martins, P.F.; Da Silva, N.D.L.; Batistella, C.B.; Maciel Filho, R.; Maciel, M.W. Simulation and cost estimate for biodiesel production using castor oil. *Chem. Eng. Res. Des.* **2010**, *88*, 626–632. [CrossRef]
8. Yang, R.; Su, M.; Zhang, J.; Jin, F.; Zha, C.; Li, M.; Hao, X. Biodiesel production from rubber seed oil using poly (sodium acrylate) supporting NaOH as a water-resistant catalyst. *Bioresour. Technol.* **2011**, *102*, 2665–2671. [CrossRef]
9. Gürü, M.; Artukoğlu, B.D.; Keskin, A.; Koca, A. Biodiesel production from waste animal fat and improvement of its characteristics by synthesized nickel and magnesium additive. *Energy Conver. Manag.* **2009**, *50*, 498–502. [CrossRef]
10. Teo, S.H.; Rashid, U.; Taufiq-Yap, Y.H. Biodiesel production from crude *Jatropha curcas* oil using calcium based mixed oxide catalysts. *Fuel* **2014**, *136*, 244–252. [CrossRef]
11. Ma, G.; Dai, L.; Liu, D.; Du, W. A robust two-step process for the efficient conversion of acidic soybean oil for biodiesel production. *Catalysts* **2018**, *8*, 527. [CrossRef]
12. Cho, H.J.; Kim, J.K.; Cho, H.J.; Yeo, Y.K. Techno-economic study of a biodiesel production from palm fatty acid distillate. *Ind. Eng. Chem. Res.* **2012**, *2*, 462–468. [CrossRef]
13. Index Mundi. Malaysia palm oil production by Year. 2017. Available online: <https://www.indexmundi.com/agriculture/?country=my&commodity=palm-oil&graph=production> (accessed on 27 December 2018).
14. Tubino, M.; Junior, J.G.R.; Bauerfeldt, G.F. Biodiesel synthesis: A study of the triglyceride methanolysis reaction with alkaline catalysts. *Catal. Commun.* **2016**, *75*, 6–12. [CrossRef]
15. Akinfalabi, S.I.; Rashid, U.; Yunus, R.; Taufiq-Yap, Y.H. Synthesis of biodiesel from palm fatty acid distillate using sulfonated palm seed cake catalyst. *Renew. Energy* **2017**, *111*, 611–619. [CrossRef]
16. Chin, L.H.; Abdullah, A.Z.; Hameed, B.H. Sugar cane bagasse as solid catalyst for synthesis of methyl esters from palm fatty acid distillate. *Chem. Eng. J.* **2012**, *183*, 104–107. [CrossRef]
17. Dehkoda, A.M.; West, A.H.; Ellis, N. Biochar based solid acid catalyst for biodiesel production. *Appl. Catal. A Gen.* **2010**, *382*, 197–204. [CrossRef]
18. Li, M.; Zheng, Y.; Chen, Y.; Zhu, X. Biodiesel production from waste cooking oil using a heterogeneous catalyst from pyrolyzed rice husk. *Bioresour. Technol.* **2014**, *154*, 345–348. [CrossRef]
19. Sani, Y.M.; Raji-Yahya, A.O.; Alaba, P.A.; Aziz, A.R.A.; Daud, W.M.A.W. Palm frond and spikelet as environmentally benign alternative solid acid catalysts for biodiesel production. *BioResources* **2015**, *10*, 3393–3408. [CrossRef]
20. Soltani, S.; Rashid, U.; Yunus, R.; Taufiq-Yap, Y.H. Biodiesel production in the presence of sulfonated mesoporous ZnAl₂O₄ catalyst via esterification of palm fatty acid distillate (PFAD). *Fuel* **2016**, *178*, 253–262. [CrossRef]
21. Cimino, S.; Lisi, L.; De Rossi, S.; Faticanti, M.; Porta, P. Methane combustion and CO oxidation on LaAl 1-x MnxO₃ perovskite-type oxide solid solutions. *Appl. Catal. B Environ.* **2003**, *43*, 397–406. [CrossRef]
22. Olutoye, M.A.; Wong, C.P.; Chin, L.H.; Hameed, B.H. Synthesis of FAME from the methanolysis of palm fatty acid distillate using highly active solid oxide acid catalyst. *Fuel Proc. Technol.* **2014**, *124*, 54–60. [CrossRef]

23. Yang, J.C.; Jablonsky, M.J.; Mays, J.W. NMR and FT-IR studies of sulfonated styrene-based homopolymers and copolymers. *Polymer* **2002**, *43*, 5125–5132. [[CrossRef](#)]
24. Farooq, M.; Ramli, A.; Subbarao, D. Biodiesel production from waste cooking oil using bifunctional heterogeneous solid catalysts. *J. Clean. Prod.* **2013**, *59*, 131–140. [[CrossRef](#)]
25. Alhassan, F.H.; Yunus, R.; Rashid, U.; Sirat, K.; Islam, A.; Lee, H.V.; Taufiq-Yap, Y.H. Production of biodiesel from mixed waste vegetable oils using ferric hydrogen sulphate as an effective reusable heterogeneous solid acid catalyst. *Appl. Catal. A Gen.* **2013**, *456*, 182–187. [[CrossRef](#)]
26. Thommes, M. Physical adsorption characterization of nanoporous materials. *Chem. Ing. Tech.* **2010**, *82*, 1059–1073. [[CrossRef](#)]
27. Xie, Z.; Liu, Z.; Wang, Y.; Yang, Q.; Xu, L.; Ding, W. An overview of recent development in composite catalysts from porous materials for various reactions and processes. *Int. J. Mol. Sci.* **2010**, *11*, 2152–2187. [[CrossRef](#)] [[PubMed](#)]
28. Kandedo, J.; Lee, K.T. Process optimization and kinetic study for biodiesel production from non-edible sea mango (*Cerbera odollam*) oil using response surface methodology. *Chem. Eng. J.* **2013**, *214*, 157–164. [[CrossRef](#)]
29. Chen, H.; Peng, B.; Wang, D.; Wang, J. Biodiesel production by the transesterification of cottonseed oil by solid acid catalysts. *Front. Chem. Eng. China* **2007**, *1*, 11–15. [[CrossRef](#)]
30. Di Serio, M.; Cozzolino, M.; Tesser, R.; Patrono, P.; Pinzari, F.; Bonelli, B.; Santacesaria, E. Vanadyl phosphate catalysts in biodiesel production. *Appl. Catal. A Gen.* **2007**, *320*, 1–7. [[CrossRef](#)]
31. Du, C.Y.; Zhao, T.S.; Liang, Z.X. Sulphonation of carbon-nanotube supported platinum catalysts for polymer electrolyte fuel cells. *J. Power Sources* **2008**, *176*, 9–15. [[CrossRef](#)]
32. Peng, F.; Zhang, L.; Wang, H.; Lv, P.; Yu, H. Sulfonated carbon nanotubes as a strong protonic acid catalyst. *Carbon* **2005**, *43*, 2405–2408. [[CrossRef](#)]
33. Upare, P.P.; Yoon, J.W.; Kim, M.Y.; Kang, H.Y.; Hwang, D.W.; Hwang, Y.K.; Kung, H.H.; Chang, J.S. Chemical conversion of biomass-derived hexose sugars to levulinic acid over sulfonic acid-functionalized graphene oxide catalysts. *Green Chem.* **2013**, *15*, 2935–2943. [[CrossRef](#)]
34. Shuit, S.H.; Lee, K.T.; Kamaruddin, A.H.; Yusup, S. Reactive extraction and in situ esterification of *Jatropha curcas* L. seeds for the production of biodiesel. *Fuel* **2010**, *89*, 527–530. [[CrossRef](#)]



© 2019 by the authors. Licensee MDPI, Basel, Switzerland. This article is an open access article distributed under the terms and conditions of the Creative Commons Attribution (CC BY) license (<http://creativecommons.org/licenses/by/4.0/>).